MDPI

Intermetallic Reaction of the Bonding Interface of TA2/Q235 Explosive Welding Composite

Qiang Zhou [1,2,*], **Honghong Lu [3]**, **Yudong Zhang [1]**, **Yansong Guo [1]**, **Lei Zhu [4]**, **Guangyan Huang [1,2]** and **Pengwan Chen [1,*]**

1 State Key Laboratory of Explosion Science and Technology, Beijing Institute of Technology, Beijing 100081, China
2 Chongqing Innovation Center, Beijing Institute of Technology, Chongqing 401120, China
3 Huanghe Science and Technology University, Zhengzhou 450000, China
4 Xi'an Tianli Metal Composite Materials Co., Ltd., Xi'an 710201, China
* Correspondence: qiangzhou886@163.com (Q.Z.); pwchen@bit.edu.cn (P.C.)

Abstract: During the explosive welding, the bonding interface of welded materials was fast heated due to high strain rate and drastic plastic deformation. The periodical wave interface, with an amplitude of ~300 μm and a period wavelength of ~800 μm, was identifiable as a uniform wave interface formed in the bonding interface. The details of the formation of melting zone and mixing zone of welding materials at the interface were observed. Combined with the Ti-Fe binary phase diagram and the principle of diffusion welding, the phase composition and evolution process of the melting and mixing zone of the bonding interface were investigated by transmission electron microscopy (TEM) and energy dispersive spectrometer (EDS). Significance of the intermetallic compound was found in the mixing zone and melting zone, which was mainly TiFe, $TiFe_2$, TiO_2, Fe_2O_3 and some other intermetallic oxides. Meanwhile, the phenomenon of the titanium agglomeration and oxygen precipitation was observed in the melting zone. The bonding interface could be determined as a mixing welding of mechanical mixing, melting, diffusion and solidification that occurred in the mixing zone, and melting welding and diffusion welding mainly occurred in the melting region.

Keywords: explosive welding; bonding interface; melting area; intermetallic reaction; microstructure evolution

1. Introduction

The metallurgically incompatible of Fe and Ti alloys often occurred in conventional fusion welding process, and the type of intermetallic compound (FeTi, Fe_2Ti) and various secondary phases would lead to embrittlement of the bonding interface [1]. Explosive welding was a special type of welding method, which could be used to weld two or more similar and dissimilar plates [2,3]. A TA2/Q235 explosive welding composite plate was widely utilized in various applications including aerospace, petrochemical, mechanical, electronics and nuclear industries [4–8]. The melting and mixing zone of the joining interface, commonly occurred in the explosive welding. In recent years, higher requirements were put forward for TA2/Q235 explosive welded joints. Different degrees of melting layer are often formed in the micro area of explosion welding interface between titanium and steel, and the high brittleness melting zone often causes the spontaneous cracking of welded joints.

The microstructure of the bonding interface was studied by many scholars. For example, Rozumek et al. [9] reported the influence of heat treatment parameters on the cracks growth under cyclic bending in St-Ti clad obtained by explosive welding. The study indicated that a higher annealing temperature results in a lower fatigue life, but for a given annealing temperature, a longer annealing time results in a higher fatigue life. Prażmowski et al. [10] reported the influence of the microstructure near the interface of the fatigue life

of explosively welded (carbon steel)/Zr clads.Li et al. [11] reported that discontinuous intermetallic including $TiFe_2$, TiFe and Ti fragments coexisted in the melted zone, and the equiaxed nanograins can be seen in the recrystallization zone and mixed zone. Zeng et al. [12] showed that the formation of oxides at the bonding interface was effectively inhibited under the helium gas during explosive welding and the mechanical properties and welding quality were improved. Wang et al. [13] showed that liquefaction occurred at the explosive interface layer in the electron beam welding process, which consisted of Fess, Fe + $TiFe_2$ eutectic, TiFe + $TiFe_2$ peritectic and Ti + $TiFe_2$ eutectic from the Fe side to the Ti side. Chu et al. [14] reported that Fe_2Ti and FeTi + Fe phases mainly formed in the melted zone. A reaction layer (~700 nm) was observed in the bonding interface. The structure of melt zone was discussed and a simple method to estimate the heating and cooling rate of bonding interface was proposed of explosive welding materials. [15] The heating rate and cooling rate at the interface were 10^9 K/s and 10^7 K/s, respectively. Zhou et al. [16] investigated the effect of microstructures on mechanical properties of TA2/Q235 bonding interface. The results showed that the defects, such as cavities, cracks and brittle intermetallic, resulted in degraded mechanical properties of the bonding interface. Many researchers indicated that the melt zone consisted of intermetallic compound, such as TiFe and $TiFe_2$. Ha [17] and Refaey [18] also indicated that the intermetallic compounds mainly were TiFe and $TiFe_2$ in Ti/STS clad welding interface. Song et al. [19] reported that the electron diffraction patterns acquired from these regions did not consider unambiguous phase identification. Above all, the researchers mainly investigated the microstructure of the bonding interface and made a qualitative analysis of the defects (cracks, intermetallic compound, cavities, etc.) in the bonding interface. Some researchers investigated the effect of microstructure of welding interface on mechanical properties. However, many scholars did not reach a clear and systematic understanding of the composition and evolution process of the melting zone and welding zone in the bonding interface.

In this work, we carried out TEM and EDS measurements to examine the phase composition of melting and mixing micro area at the TA2/Q235 bonding interface. In order to explore the interfacial reaction mechanism, combined with the Ti-Fe binary phase diagram and the principle of diffusion welding, the phase composition and evolution process of the melting and mixing zone of the welding interface were reported. This was very important for increasing the strength of the welding interface.

2. Materials and Methods

2.1. Materials Preparation

Figure 1 showed the schematic diagram of the explosive welding process. It can be observed in Figure 1 that a mild steel plate (Q235) was parallel placed under a commercial purity titanium plate (TA2), the dimension of which was 600 × 300 × 15 mm and 600 × 300 × 5 mm, respectively. Tables 1 and 2 showed the chemical composition and mechanical properties of the welding materials.
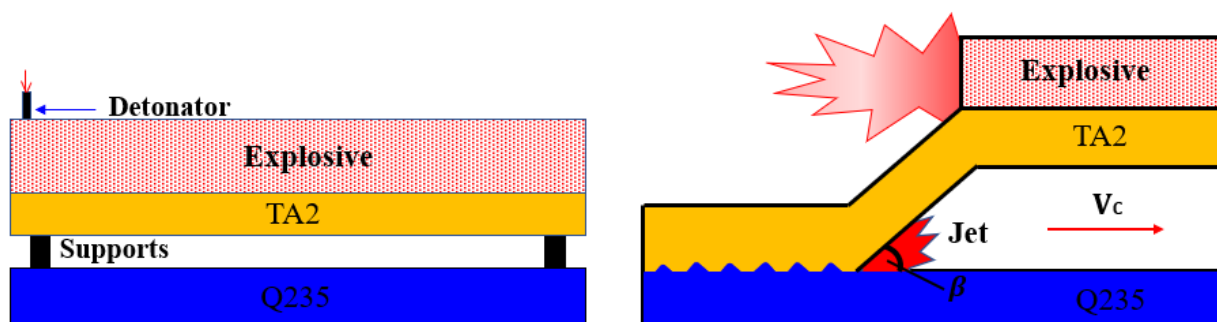

Figure 1. Schematic of the explosive welding device.

Table 1. Chemical composition of the welding materials. (Mass fraction, %) [20].

Material	Fe	Ti	C	Si	S	P	Mn	O	N
TA2	0.06	Bal.	0.01	-	-	-	-	0.126	0.01
Q235	Bal. (1)	-	0.22	0.35	0.045	0.045	1.4	-	-

Table 2. Mechanical properties of the welding plates [21].

Samples	Elastic Modulus, GPa	Yield Strength, MPa	Tensile Strength, MPa	Elongation, %
TA2	103	373	440–590	25
Q235	210	235	372–510	26

During the welding process, the flyer plate and base plate collided at an angle β. The following equation showed the relationship between the collision velocity V_C and the impact velocity V_P: [22]

$$V_C = \frac{V_P}{2sin\frac{\beta}{2}} \tag{1}$$

Equation (2) can calculate the collision angle β [23].

$$\beta = \left(\sqrt{\frac{k+1}{k-1}} - 1\right) \cdot \frac{\pi}{2} \cdot \frac{r}{r + 2.71 + 0.184t_e/s} \tag{2}$$

where t_e is the explosive thickness, r is the loading ratio (the unit of the explosive mass divide flyer plate mass,1.7), s is the stand-off distance (10 mm) and k is a constant with a range of 1.81 to 2.6 based on the explosive thickness, [24]. An ammonium nitrate fuel oil (ANFO) mixture was chosen as the explosive material with a density of 0.92 g/cm^3. The detonation velocity was 2600 m/s, the thickness was 40 mm, the collision angle was 22° and the collision velocity was 997 m/s.

2.2. Microstructure Characterization

The microstructure of the bonding interface was observed by the metallographic specimens. The metallographic specimens were cut from the central part in the bonding interface along the detonation direction. Then, the standard mechanical polishing and etching the 5% nitric acid and 95% ethyl alcohol (by volume) mixture were carried out. The microstructures of bonding interface were characterized with LEICA DMI 3000 M optical microscope (OM) from Tongzhou Tongde (Beijing) Instrument Co., LTD made in China. Transmission electron microscopy (TEM) and energy dispersive spectrometer (EDS) detectors were performed with the FEI Tecnai G2-F30 (from Japan Electronics Corporation made in Japan) to investigate microstructure evolution and chemical distribution in the bonding interface, respectively.

2.3. Ti-Fe Binary Phase Diagram

In Figure 2, according to the analysis of binary alloy phase in the melting zone, there were two main mesophase formed in the bonding interface between Fe and Ti, which were TiFe (cubic crystal structure) and TiFe$_2$ (hexagonal crystal structure). When the temperature was 200 °C, the composition structure remained the same as the original. At 250 °C, mutual diffusion occurred in sublayers between Fe and Ti, and the composition modulation structure was destroyed, but no phase transition occurred. When the temperature reached 350 °C, supersaturated solid solution α-Fe(Ti) and intermetallic compound TiFe were formed [25]. The formation of Ti/Fe intermetallic compound depended on the initial Fe and Ti sublayer diffusion. At about 13 at.% Fe at 590 °C, the β-Ti phase occurred eutectoid

decomposition (β-Ti) ⇌ (α-Ti) + TiFe. The liquid phase only existed in a small area at the Ti-Fe interface in the range of 1000 °C–1100 °C, forming a narrow eutectic reaction zone. At 1085 °C, eutectic reaction occurred at about 29 at.% Fe, L ⇌ (β-Ti) + TiFe. At 1289 °C, the eutectic reaction occurred at 84% Fe (Atom Fraction), L ⇌ (α-Ti) + TiFe. TiFe was formed by peritectic reaction at 1317 °C, L + TiFe₂ ⇌ TiFe. Intermetallic TiFe was firstly formed in TA2/Q235 interface at higher annealing temperature [26,27]. Intermetallic TiFe₂ formed between intermetallic TiFe and the excessive Fe at 1427 °C.
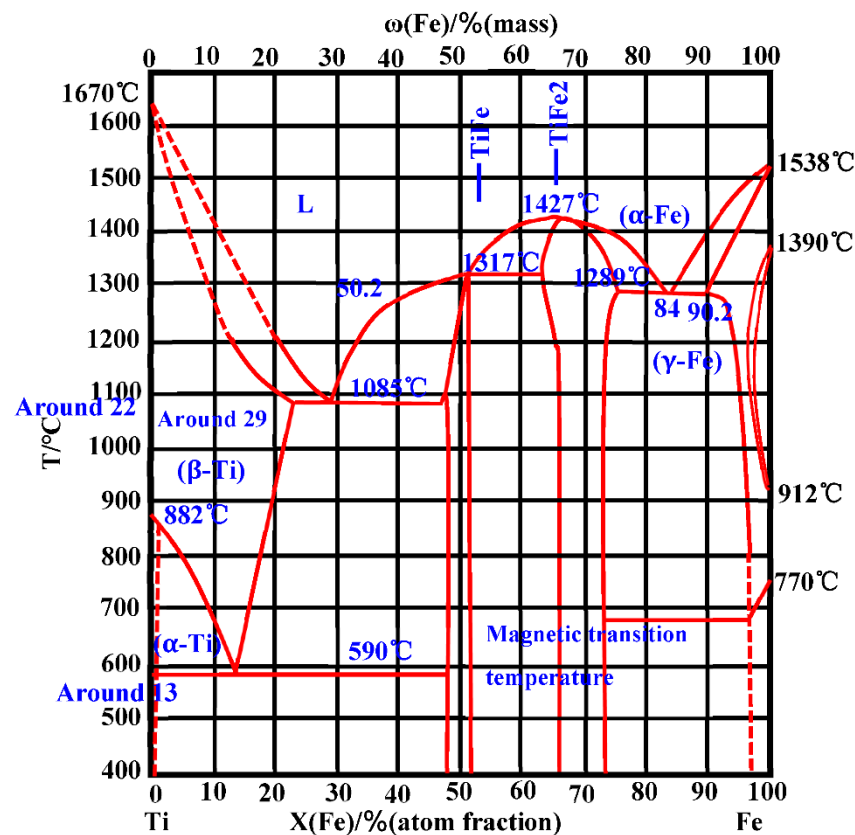

Figure 2. Ti-Fe binary phase diagram [28].

Combined with the above research analysis of Ti-Fe binary phase diagram, the formation process and mechanism of Ti/Fe intermetallic compound in the bonding interface could be evaluated and analyzed.

3. Results and Discussion

3.1. Microstructure of the Welding Interface

Figure 3 displayed the typical microstructure of the TA2/Q235 welding interface. It could be seen from Figure 3 that the bonding interface presented a periodical wave interface, the amplitude and period wavelength was ~300 μm and ~800 μm, respectively. Bataev et al. [15] reported that the formation of the wavy interface was the result of the change of the pressure distribution at the collision point, which was caused by the self-excited oscillation in the bond region. The grains were greatly elongated in the Q235 side along the detonation direction, which showed the drastic deformation occurred at the interface in the process of explosive welding. The mechanisms of hydromechanics in the melting pool indicated that the intermetallic compounds formed in the first stage of melting moved into the wave front due to mass transfer in vortex flows. The temperature gradient, liquid and partially solid mixing of materials due to wave detonation and the serve plastic deformations in the joint zone were the main causes of structural inhomogeneity. Furthermore, some defects (microcracks, voids and intermetallic compound) were mainly formed in the vortex of

the bonding interface. It should be noted that the intermetallic phase was mainly formed between dissimilar metals [14]. The high temperature and high pressure were generated at the collision point due to the collision between flyer plate and base plate. The dissipation of kinetic energy was accompanied by a rapid temperature boost and the melted zones was formed in the bonding interface.
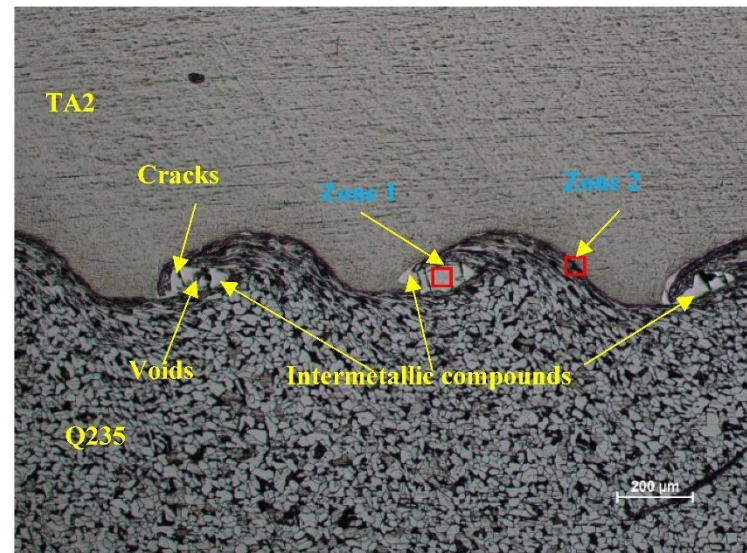

Figure 3. Typical microstructure of the welding interface.

Bataev et al. [15] indicated that the heating rate could reach 10^9 K/s. The result was consistent with Crossland [29] and Kacar [30]. Meanwhile, Gloc [31] indicated that voids and intermetallic compounds were always formed in the welding interface because the heat was not dissipated in time. This would result in the initiation of cracks due to the poor toughness and inner stress in the welding interface. In order to further evaluate the evolution and formation process of intermetallic compounds and the diffusion between Ti and Fe elements in the bonding interface. In Figure 3, zone 1 and zone 2 were selected as the area to study.

3.2. TEM and EDS Analysis of the Melting Zone

Figure 4 showed TEM and EDS result of melting zone of the crest at the TA2/Q235 bonding interface, which could be used to investigate the phase composition distribution in the melting area. As seen in Figure 4a,b, the TEM lamella was prepared perpendicular to the bonding interface by focused ion beam (FIB). Figure 4c displayed heterogeneous phases in the bright-field TEM image of the melting zone. It was suggested that mechanical mixing, melting, diffusion and solidification occurred concurrently forming the complex structure [11]. Moreover, EDS line scanning and EDS map scanning under the TEM bright field were carried out, as illustrated in Figure 4c,d. Figure 4c showed that heterogeneous titanium islands were found in the mixing zone. Li et al. [11] reported that the formation of heterogeneous titanium islands was due to the mechanical mixing happened in the welding interface. Then, melting and mixing of materials in the crest occurred afterwards due to high temperature and severe plastic deformation. Then, the diffusion occurred in the melted zone during the process of solidification. Figure 4f showed that the precipitation agglomeration reaction of oxygen occurred in the mixing zone. The presence of oxygen in the reaction was unavoidable, because explosive welding took place in the air.
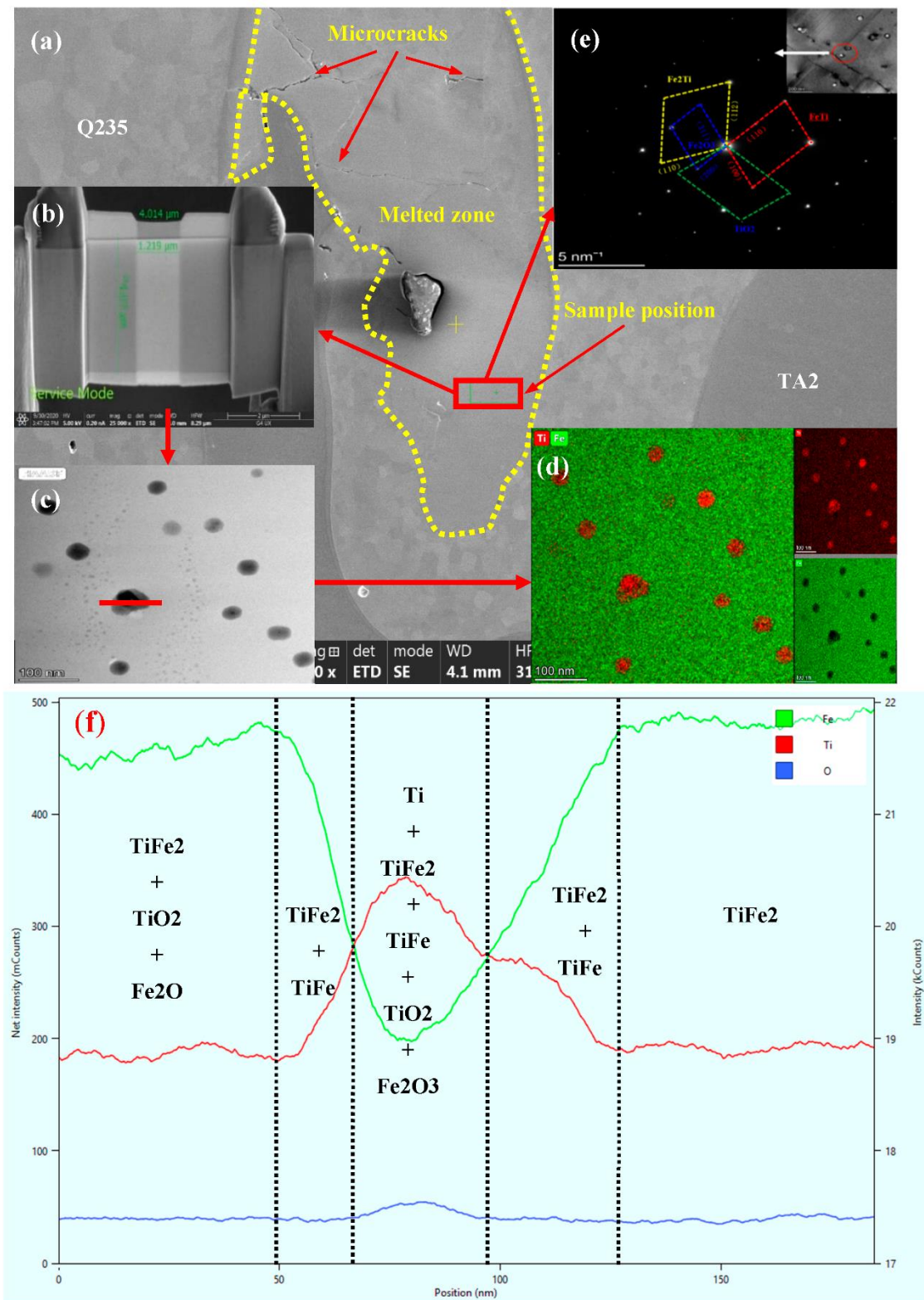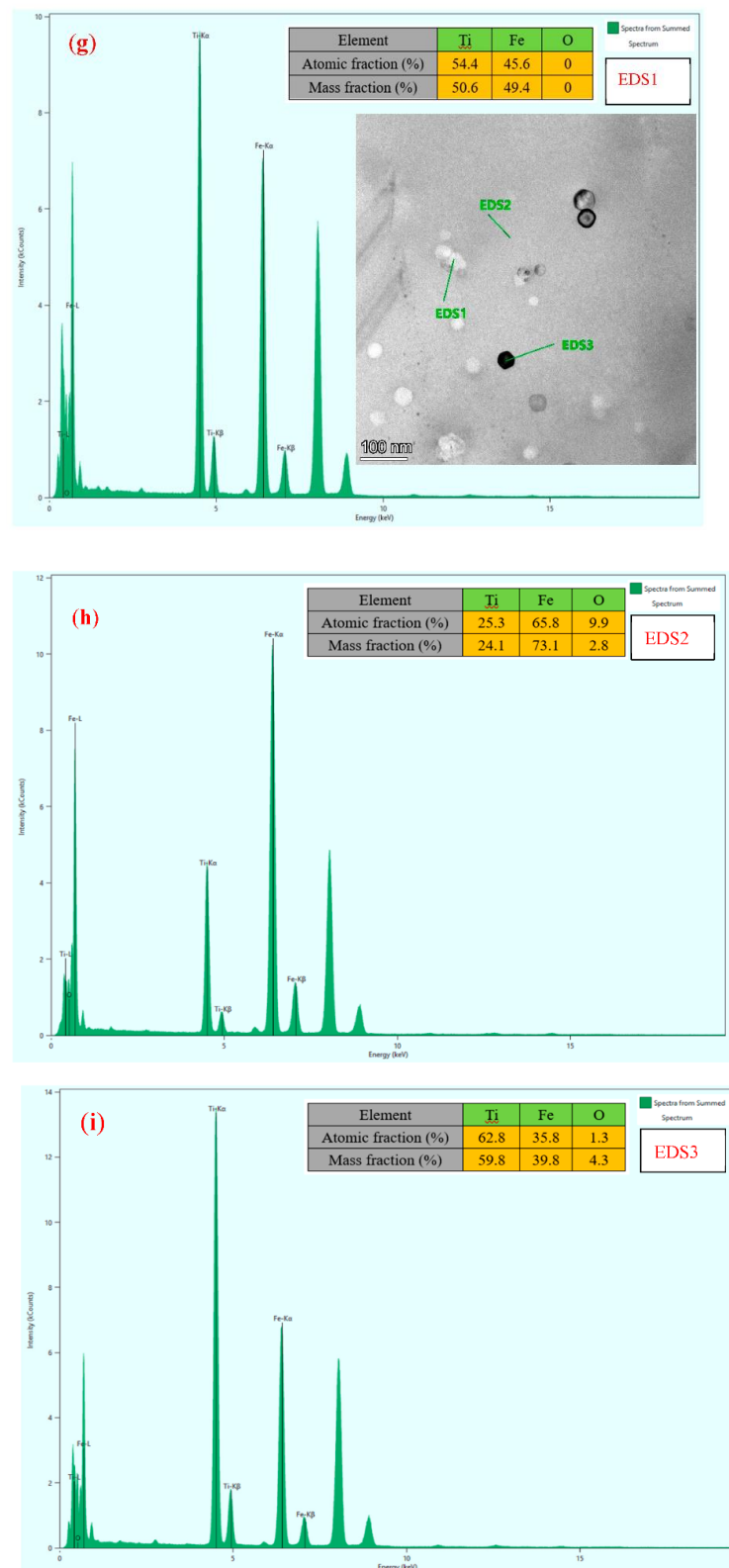
Figure 4. *Cont.*

Figure 4. TEM result of melting zone of the crest at the TA2/Q235 interface: (**a**) TEM sample cut perpendicular to the melting zone; (**b**) TEM sample prepared by FIB; (**c**) TEM bright field image; (**d**) EDS map scanning under the TEM bright field; (**e**) the selected area electro diffraction (SAED) showing formation of different phase in the melting region; (**f**) EDS line scanning under the TEM bright field; (**g**) EDS1 point scanning, (**h**) EDS2 point scanning and (**i**) EDS3 point scanning under the TEM bright field.

The selected area electro diffraction (SAED) was performed in the mixing zone, as shown in Figure 4e. It could be seen that nano-grained intermetallic phase formed in the melting zone, which was mainly consisted of TiFe, $TiFe_2$ and part of Ti and Fe oxide through the analysis of the selected area diffraction pattern.

Meanwhile, Figure 4 showed the EDS analysis results of elemental points 1~3. It indicated that the precipitation agglomeration reaction of different phase titanium occurred in the mixing zone. For the mixing zone in white zone with EDS 1, the compositions were 49.4 wt.% Fe, 50.6 wt.% Ti, 0 wt.% O; 45.6 at.% Fe, 54.4 at.% Ti, 0 at.% O, as seen in Figure 4g. It was determined to be mainly composed of FeTi, α-Ti, β-Ti, α-Fe, β-Fe. Eutectoid decomposition or eutectic reaction mainly occurred in this region, (β-Ti) $\rightleftharpoons$ (α-Ti) + TiFe, L $\rightleftharpoons$ (α-Ti) + TiFe.

For the melting zone in grey with EDS 2, the compositions were 49.4 wt.% Fe, 50.6 wt.% Ti, 2.8 wt.% O; 45.6 at.% Fe, 54.4 at.% Ti, 9.9 at.% O, as shown in Figure 4h. During the explosive welding, the high-speed collisions at the joint of the two plates occurred with high temperature and high pressure, the temperature quickly increased in the interface. At higher temperatures, the heat energy provided to the diffusing atoms permitted the atoms to overcome the activation energy barrier and move more easily to the mixing zone. The limitation of Fe and Ti atomic concentration led to a mixture of intermetallic TiFe and $TiFe_2$ [32]. Thus, the phenomenon of heterogeneous titanium islands occurred in regions of EDS 1 and EDS 3. Therefore, it can be determined to be mainly composed of $TiFe_2$, TiFe, α-Ti, β-Ti, α-Fe, β-Fe and some metal oxides (such as TiO_2, Fe_2O_3) in the mixing zone. $TiFe_2$ is a stable compound, and so, the solid and liquid melted with the same composition at 1427 °C. As the temperature decreased, peritectic reaction: L + $TiFe_2$ $\rightleftharpoons$ TiFe, eutectic reaction: L $\rightleftharpoons$ (α-Ti) + TiFe and L $\rightleftharpoons$ (β-Ti) + TiFe, eutectoid decomposition: (β-Ti) $\rightleftharpoons$ (α-Ti) + TiFe may have occurred in different regions.

For the melting zone in black with EDS 3, the compositions were 59.8 wt.% Fe, 39.8 wt.% Ti, 4.3 wt.% O; 35.8 at.% Fe, 62.8 at.% Ti, 1.3 at.% O, as seen in Figure 4i. It was determined to be mainly composed of $TiFe_2$, TiFe, α-Ti, β-Ti, α-Fe, β-Fe and some metal oxides (such as TiO_2, Fe_2O_3), as seen in Figure 4h. Eutectic reaction mainly occurred in this region, L $\rightleftharpoons$ (β-Ti) + TiFe, L $\rightleftharpoons$ (α-Ti) + TiFe, L + $TiFe_2$ $\rightleftharpoons$ TiFe.

3.3. TEM and EDS Analysis of the Welding Zone

Combined with the results of our previous research, the TEM was carried out to further investigate the microstructure in the welding zone, as shown in Figure 5. This could be used to determine the microstructure evolution of bonding interface during the explosive welding. Figure 5a showed that the TEM sample was prepared by the FIB method. The bright-field TEM image of the melting zone was shown in Figure 5b. It could be seen from Figure 5b that a reaction layer about 300 nm thickness formed in the melting zone. Chu et al. [14] indicated that the reaction layer was composed of very fine grains (nano-size) with the diameter rarely exceeding 200 nm. The obvious diffusion layer that existed at the interface could be seen from the EDS map scanning, as illustrated in Figure 5c. Figure 5d displayed the selected area electro diffraction (SAED) of the melting zone, TiFe, $TiFe_2$, Ti and part of Ti and Fe oxide (TiO_2, $Fe_{0.90}O$ and Fe_2O_3) were formed in the melting zone. A similar structure of the bonding interface was reported by Song et al. [19] and Paul et al. [33]. However, the reaction layer made a good bonding between the flyer plate and base plate [16]. Therefore, the thin reaction layer was probably essential to improve the bonding strength of welding interface. Above all, melting welding and diffusion welding mainly occurred in the melting region.
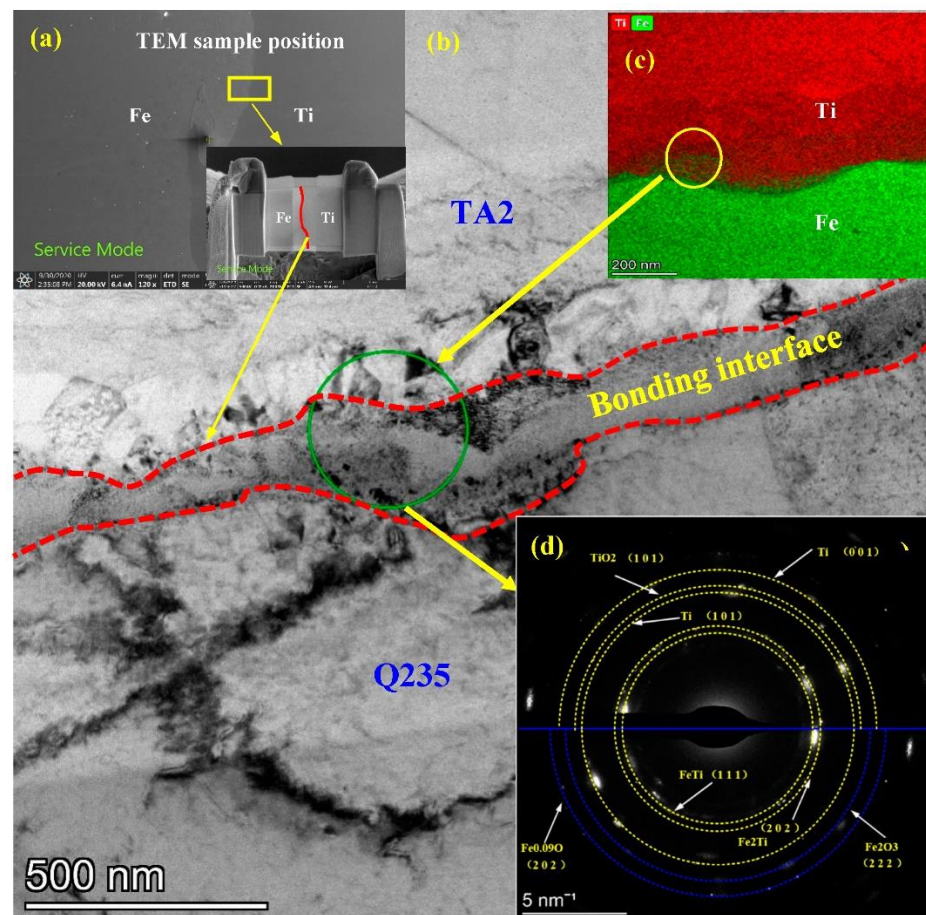
Figure 5. TEM result at the TA2-Q235 interface: (**a**) TEM sample cut perpendicular to the Ti/Fe interface and prepared by FIB; (**b**) TEM bright field image; (**c**) EDS map scanning under the TEM bright field; (**d**) the selected area electro diffraction (SAED) showing formation of nano-grained intermetallic phase in the interface region [16].

The bonding mode of explosive welding interface can be regarded as diffusion welding under the conditions of high temperature, high pressure and large deformation of the base material. Figure 5 presented the growth process of the reaction layer of the bonding interface during explosive welding. β-Ti solid solution and Ti-Fe intermetallic compound formed at the TA2-Q235 interface. The formation of β-Ti solid solution occurred near the TA2 side. The β-Ti + TiFe eutectic formed in the middle of the TA2-Q235 bonding interface. $TiFe_2$ phase was formed near the Q235 side. Zhang et al. [34] highlighted that bonding interface was divided into β-Ti solid solution being on the Ti side, β-Ti + TiFe eutectic in the middle of the interface zone and $TiFe_2$ phase being on the Fe side. In addition, when a small amount of Fe diffused into the liquid phase on the Ti side, β-Ti solid solution was formed. $TiFe_2$ phase was formed when Ti diffused to the Fe side and dissolved into Fe. Wang et al. [35] reported that Fe/Ti had an interlaminar diffusion process before the formation of intermetallic compounds. TA2/Q235 bonding interface thermal instability processes include interlaminar diffusion and the formation and growth of TiFe intermetallic compound. The regulation of TA2-Q235 nanostructures is controlled by thermodynamic and kinetic factors [27,32].

As per the above analysis, the interfacial reaction layer was mainly β-Ti solid solution, TiFe and $TiFe_2$ compounds. The formation of intermetallic compounds was primarily determined by thermodynamic factors. Ti-Fe intermetallic was formed due to the temperature increase in the TA2-Q235 bonding interface in the explosive welding. It was well known that the growing Gibbs free energy ΔG was a relative quantity in the classical physicochemical theory. It provided a method to study the possibility to the formation of

Ti-Fe intermetallic by the thermodynamic analysis. The standard free energy could be used to evaluate the free energy of each substance in Equation (3):

$$\Delta G_T^{\Theta} = \Delta H_T^{\Theta} - T\Delta S_T \tag{3}$$

where T was reaction temperature; ΔG_T^{Θ} was standard reaction Gibbs free energy; ΔH_T^{Θ} was reaction enthalpy change and $T\Delta S_T$ was the reaction entropy change. When $\Delta G_T^{\Theta} < 0$, the reaction was spontaneous; when $\Delta G_T^{\Theta} \geq 0$, the reaction could not occur spontaneously. Zhang et al. [34] reported that the range of the standard Gibbs free energy G of Ti-Fe intermetallic compound was 400 °C~1600 °C, as shown in Figure 6. The reaction free energy of TiFe could reach -100 kJ/mol, the temperature was more than 1000 °C. At the same temperature, TiFe$_2$ phase reaction free energy could reach -300 kJ/mol. Which indicated that the two reactions were extremely easy to generate in the welding process. Meanwhile, TiFe$_2$ phase was much easier to generate in the cooling crystallization process.
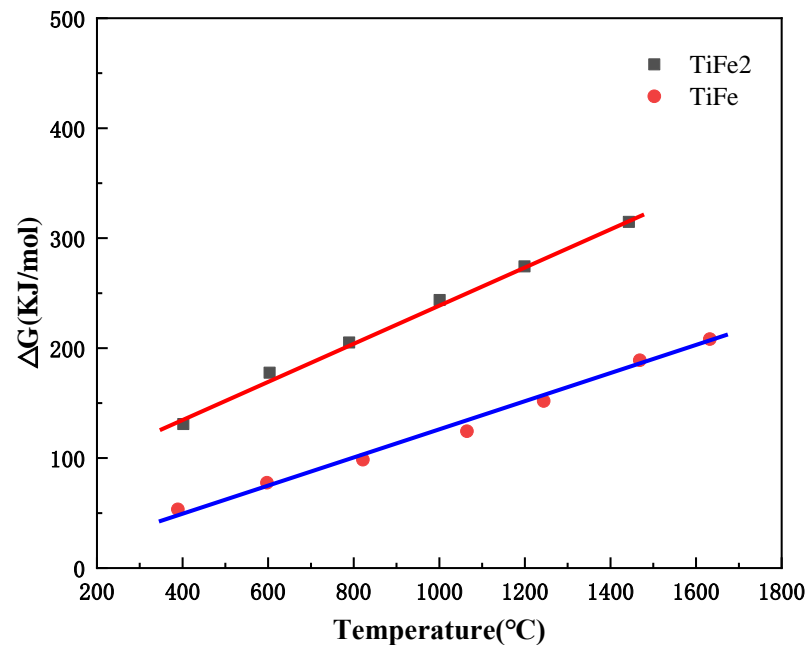

Figure 6. Temperature—Gibbs free energy curve of TiFe and TiFe$_2$.

Figure 7 showed the formation process of reaction layer in the welding interface. During explosive welding, eutectic liquid phase of the matrix material was generated at the interface, because the TA2-Q235 interface temperature increased, and the element diffusion happened simultaneously, as shown in Figure 7a. β-Ti + TiFe eutectic structure at the interface were mainly precipitated from the liquid during cooling in Figure 7b. In the process of cooling crystallization of the reaction layer, the heat of TA2-Q235 welding interface primarily originated from the thermal conduction of TA2. Moreover, the temperature of the Q235 side decreased faster because the heat conductivity of Q235 was greater than that of TA2. Furthermore, the temperature gradient was formed in the reaction area. The β-Ti solid solution was first formed because the highest heat was obtained on the TA2 side. Yu et al. [36] indicated that β-Ti solid solution was mainly formed on the TA2 side due to the dissolution rate of Ti was higher than Fe. Cao et al. [37] reported that the direction perpendicular to the solid/liquid interface presented the highest temperature gradient, which induced the formation of the coarse columnar β-Ti grains.
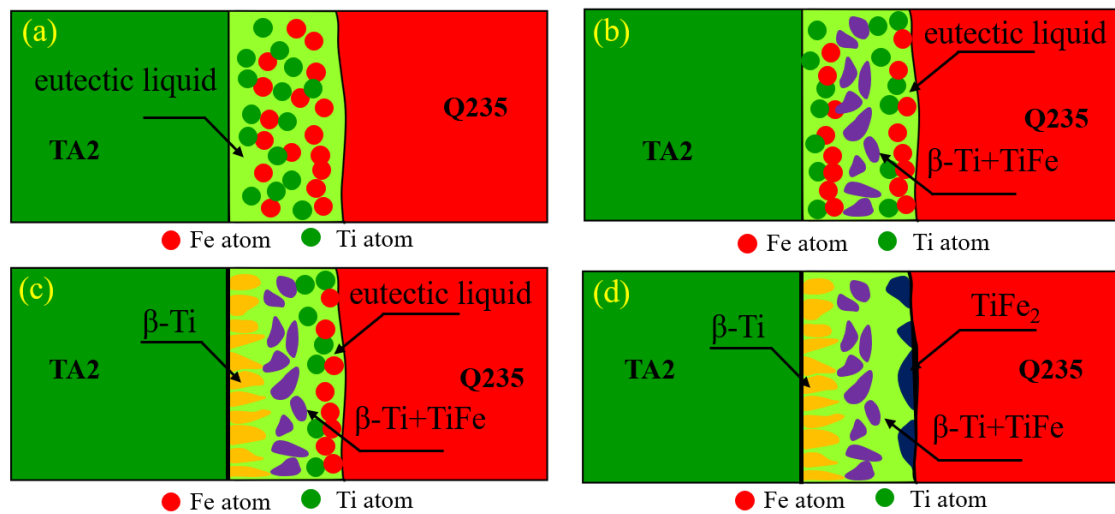
Figure 7. Growth process of the reaction layer during explosive welding: (**a**) dissolution and diffusion of Ti and Fe in the interface; (**b**) nucleation and growth of β-Ti + TiFe eutectic; (**c**) formation of solid-phase reaction layer at TA2 side; (**d**) formation of TiFe$_2$ in the solid-phase reaction layer at Q235 side.

As the Ti-Fe binary phase diagram suggested, the solubility of Ti atom in Fe atom was 10 at.% [38]. Ti-Fe intermetallic compounds were mainly produced near the Q235 side, and β-Ti was mainly produced near the TA2 side. The formation of reaction layer was controlled by the rate of Ti and Fe atoms diffusion. Fe in the liquid phase diffused into TA2 as the solid phase into the eutectic liquid phase, the reaction layer would be formed, as shown in Figure 7c. Simultaneously, another solid-phase diffusion layer would be formed as Ti in the liquid phase diffused into Fe, as shown in Figure 7d.

In the liquid phase, due to the relatively small diffusion coefficient of Ti atoms, titanium atoms could obtain enough iron atoms to be combined with, which was easy to form TiFe$_2$ phase. Therefore, the diffusion of Ti atoms in SS quickly reached the solubility limit of iron based solid solution, which formed TiFe$_2$ phase. The reaction layer would be formed after the liquid phase was solidified.

In the process of explosive welding, the nucleation and growth of the reaction layer were determined by the diffusion rate and atomic concentration of Ti and Fe atoms. The growth rate and thickness of the compound in the welding interface were determined by the maximum temperature and the cooling rate of TA2 side [39].

As the analysis suggests, dissolution and diffusion of Ti and Fe played a major role in the formation of the interfacial reaction layer. The diffusion of Ti and Fe atoms controlled the formation of the reaction layer. The formation of intermetallic compounds was secondly influenced by kinetic factors. The thickness of intermetallic compound layer could be expressed as the function of X in Equation (4).

$$X = K{\cdot}exp\left(-\frac{Q}{RT}\right)t^n \tag{4}$$

K is constant, Q is the diffusion activation energy, t is reaction time, T is the reaction temperature, n is time factor (0.5) and R is the gas constant (R = 8.314 J/(mol·K)). Equation (4) suggests that the T and t have an obvious effect on the formation of intermetallic compound layer. As mentioned above, in the welding, there was a faster heating and cooling rate so that the reaction layer formed only in a narrower region of the TA2-Q235 interface. The thickness of the reaction layer can be kept comparatively low to obtain a small amount of intermetallic by reasonably controlling explosive welding parameters [40]. It contributed to improving the mechanical properties of the bonding interface.

4. Conclusions

In this paper, TA2/Q235 plate was fabricated successfully by explosive welding method. Microstructure of the melting zone and bonding interface was investigated. Combined with the Ti-Fe binary phase diagram and the principle of diffusion welding, the phase composition and evolution process of the melting and mixing zone of the bonding interface were reported. The following conclusions can be drawn:

1. The bonding interface presented a periodical wave interface, the amplitude and period wavelength was ~300 μm and ~800 μm, respectively. Moreover, some defects, such as voids, microcracks and brittle solidified materials, were formed in the vortex of the bonding zone, where the defects were mainly located in the vortex.
2. Nano-grained intermetallic phase formed in the melting zone, which was mainly consisted of TiFe, $TiFe_2$ and part of Ti and Fe oxide (TiO_2 and Fe_2O_3), and the precipitation agglomeration reaction of different phase titanium occurred in the melting zone.
3. The formation of the reaction layer was probably essential to improve the bonding strength of welding interface. Melting welding and diffusion welding mainly occurred in the melting region, which mainly consisted of TiFe, $TiFe_2$, Ti and part of Ti and Fe oxide (TiO_2, $Fe_{0.90}O$ and Fe_2O_3) in the melting region.
4. Combined with the Ti-Fe binary phase diagram and the principle of diffusion welding, the bonding of the welding interface could be determined as a mixing welding of mechanical mixing, melting, diffusion and solidification that occurred in the mixing zone, and melting welding and diffusion welding mainly occurred in the melting region.

Author Contributions: Conceptualization, P.C. and Q.Z.; methodology, P.C., Q.Z.; formal analysis, P.C., Q.Z.; investigation, P.C., Q.Z.; resources, P.C., Q.Z.; data curation, H.L., Y.Z., Y.G., L.Z.; writing—original draft preparation, Q.Z.; writing—review and editing, P.C., G.H.; supervision, P.C., G.H.; project administration, P.C.; funding acquisition, P.C., Q.Z.; All authors have read and agreed to the published version of the manuscript.

References

1. Prasanthi, T.; Sudha, R.C.; Saroja, S. Explosive cladding and post-weld heat treatment of mild steel and titanium. *Mater. Des.* **2016**, *93*, 180–193. [CrossRef]
2. Gulenc, B. Investigation of interface properties and weldability of aluminum and copper plates by explosive welding method. *Mater. Des.* **2008**, *29*, 275–278. [CrossRef]
3. Kahraman, N.; Gülenç, B. Microstructural and mechanical properties of Cu–Ti plates bonded through explosive welding process. *J. Mater. Process. Technol.* **2005**, *169*, 67–71. [CrossRef]
4. Findik, F. Recent developments in explosive welding. *Mater. Des.* **2011**, *32*, 1081–1093. [CrossRef]
5. Kundu, S.; Chatterjee, S. Diffusion bonding between commercially pure titanium and micro-duplex stainless steel. *Mater. Sci. Eng. A* **2008**, *480*, 316–322. [CrossRef]
6. Hao, X.; Dong, H.; Xia, Y.; Li, P. Microstructure and mechanical properties of laser welded TC4 titanium alloy/304 stainless steel joint with $(CoCrFeNi)_{100-x}Cu_x$ high-entropy alloy interlayer. *J. Alloys Compd.* **2019**, *803*, 649–657. [CrossRef]
7. Xia, Y.; Dong, H.; Hao, X.; Li, P.; Li, S. Vacuum brazing of Ti6Al4V alloy to 316L stainless steel using a Ti-Cu-based amorphous filler metal. *J. Mater. Process. Technol.* **2019**, *269*, 35–44. [CrossRef]

8.　Borchers, C.; Lenz, M.; Deutges, M.; Klein, H.; Gärtner, F.; Hammerschmidt, M.; Kreye, H. Microstructure and mechanical properties ofmedium-carbon steel bonded on low-carbon steel by explosive welding. *Mater. Des.* **2016**, *89*, 369–376. [CrossRef]

9.　Rozumek, D.; Kwiatkowski, G. The influence of heat treatment parameters on the cracks growth under cyclic bending in St-Ti clad obtained by explosive welding. *Metals* **2019**, *9*, 338. [CrossRef]

10.　Prażmowski, M.; Paul, H.; Rozumek, D.; Marcisz, E. Influence of the microstructure near the interface of the fatigue life of explosively welded (carbon steel)/Zr clads. *Key Eng. Mater.* **2014**, *592–593*, 704–707. [CrossRef]

11.　Li, J.; Schneiderman, B.; Gilbert, S.M.; Vivek, A.; Yu, Z.; Daehn, G. Process characteristics and interfacial microstructure in spot impact welding of titanium to stainless steel. *J. Manuf. Process.* **2020**, *50*, 421–429. [CrossRef]

12.　Zeng, X.-Y.; Wang, Y.-X.; Li, X.-Q.; Li, X.-J.; Zhao, T.-J. Effects of gaseous media on interfacial microstructure and mechanical properties of titanium/steel explosive welded composite plate. *Fusion Eng. Des.* **2019**, *148*, 111292. [CrossRef]

13.　Wang, T.; Zhang, F.; Li, X.; Jiang, S.; Feng, J. Interfacial evolution of explosively welded titanium/steel joint under subsequent EBW process. *J. Mater. Process. Technol.* **2018**, *261*, 24–30. [CrossRef]

14.　Chu, Q.; Zhang, M.; Li, J.; Yan, C. Experimental and numerical investigation of microstructure and mechanical behavior of titanium/steel interfaces prepared by explosive welding. *Mater. Sci. Eng. A* **2017**, *689*, 323–331. [CrossRef]

15.　Bataev, I.A.; Lazurenko, D.V.; Tanaka, S.; Hokamoto, K.; Bataev, A.A.; Guo, Y.; Jorge, A.M., Jr. High cooling rates and metastable phases at the interfaces of explosively welded materials. *Acta Mater.* **2017**, *135*, 277–289. [CrossRef]

16.　Zhou, Q.; Liu, R.; Chen, P.; Zhu, L. Microstructure characterization and tensile shear failure mechanism of the bonding interface of explosively welded titanium-steel composite. *Mater. Sci. Eng. A* **2021**, *820*, 141559. [CrossRef]

17.　Ha, J.S.; Hong, S.I. Deformation and fracture of Ti/439 stainless steel clad composite at intermediate temperatures. *Mater. Sci. Eng. A* **2016**, *651*, 805–809. [CrossRef]

18.　El Refaey, A.; Tillmann, W. Characterization of Titanium/Steel joints brazed in vacuum. *Weld. J.* **2008**, *87*, 113–118.

19.　Song, J.; Kostka, A.; Veehmayer, M.; Raabe, D. Hierarchical microstructure of explosive joints: Example of titanium to steel cladding. *Mater. Sci. Eng. A* **2011**, *528*, 2641–2647. [CrossRef]

20.　Yang, M.; Ma, H.; Shen, Z.; Huang, Z.; Tian, Q.; Tian, J. Dissimilar material welding of tantalum foil and Q235 steel plate using improved explosive welding technique. *Mater. Des.* **2019**, *186*, 108348. [CrossRef]

21.　Zhou, Q.; Liu, R.; Ran, C.; Fan, K.; Xie, J.; Chen, P. Effect of microstructure on mechanical properties of titanium-steel explosive welding interface. *Mater. Sci. Eng. A* **2022**, *830*, 142260. [CrossRef]

22.　Blazynski, T.Z.E. (Ed.) *Explosive Welding, Forming and Compaction*; Springer: Dordrecht, The Netherlands, 2012; ISBN (1983) 978-94-011-9753-3.

23.　Manikandan, P.; Hokamoto, K.; Deribas, A.A.; Raghukandan, K.; Tomoshige, R. Explosive Welding of Titanium/Stainless Steel by Controlling Energetic Conditions. *Mater. Trans.* **2006**, *47*, 2049–2055. [CrossRef]

24.　Liu, K.; Chen, P.; Feng, J.; Ran, C.; Wang, Y.; Zhou, Q.; Zhu, L. Fabrication and characterization of the Mo/cu bimetal with thick Mo layer and high interfacial strength. *Int. J. Refract. Met. Hard Mater.* **2020**, *94*, 105383. [CrossRef]

25.　Chen, T.; Wu, Z.L.; Cao, B.S.; Gao, J.; Lei, M.K. Solid state reaction of Fe/Ti nanometer-scale multilayers. *Surf. Coat. Technol.* **2007**, *201*, 5059–5062. [CrossRef]

26.　Lei, M.; Wu, Z.; Chen, T.; Cao, B. Microstructural evolution of Fe/Ti multilayers submitted to in situ thermal annealing. *Thin Solid Films* **2006**, *500*, 174–179. [CrossRef]

27.　Tanaka, M.O.K. Structural change of Fe:Ti multilayer during annealing in vacuum and hydrogen atmosphere. *Int. J. Hydrogen Energy* **1999**, *24*, 891–898. [CrossRef]

28.　Guo, Q.; Wang, G.; Guo, G. *Phase Atlas of Common Non—Ferrous Binary Alloys*; Chemical Industrial Press: Beijing, China, 2010.

29.　Crossland, B. *Explosive Welding of Metals and Its Application*; Clarendon Press: Oxford, UK, 1982.

30.　Kacar, R.; Acarer, M. An investigation on the explosive cladding of 316L stainless steel-din-P355GH steel. *J. Mater. Process. Technol.* **2004**, *152*, 91–96. [CrossRef]

31.　Gloc, M.; Wachowski, M.; Plocinski, T.; Kurzydlowski, K.J. Microstructural and microanalysis investigations of bond titanium grade1/low alloy steel st52-3N obtained by explosive welding. *J. Alloys Compd.* **2016**, *671*, 446–451. [CrossRef]

32.　Wu, Z.L.; Peng, T.X.; Cao, B.S.; Lei, M.K. X-ray diffraction and high resolution transmission electron microscopy characterization of intermetallics formed in Fe/Ti nanometer-scale multilayers during thermal annealing. *Thin Solid Film.* **2009**, *517*, 6553–6557. [CrossRef]

33.　Paul, H.; Morgiel, J.; Baudin, T.; Brisset, F.; Prażmowski, M.; Miszczyk, M. Characterization of Explosive Weld Joints by TEM and SEM/EBSD. *Arch. Met. Mater.* **2014**, *59*, 1129–1136. [CrossRef]

34.　Zhang, Y.; Zhou, J.; Sun, D.; Gu, X. Nd:YAG laser welding of dissimilar metals of titanium alloy to stainless steel without filler metal based on a hybrid connection mechanism. *J. Mater. Res. Technol.* **2020**, *9*, 1662–1672. [CrossRef]

35.　Wang, W.H.; Bai, H.Y.; Zhang, M.; Zhao, J.H.; Zhang, X.Y.; Wang, W.K. Interdiffusion in nanometer-scale multilayers investigated by in situ low-angle x-ray diffraction. *Phys. Rev. B* **1999**, *59*, 10811. [CrossRef]

36.　Yu, C.; Wu, M.F.; Lu, H. Factors influencing formation and growth of coarse Ti Fe compound in Ti Fe eutectic reaction. *Sci. Technol. Weld. Join.* **2006**, *11*, 265–270. [CrossRef]

37.　Cao, R.; Feng, Z.; Lin, Q.; Chen, J. Study on cold metal transfer welding–brazing of titanium to copper. *Mater. Des.* **2013**, *56*, 165–173. [CrossRef]

38.　Murray, J.L. The Fe-Ti (Iron-Titanium) system. *Bull. Alloy. Phase Diagr.* **1981**, *2*, 320–334. [CrossRef]

39. Kundu, S.; Ghosh, M.; Laik, A.; Bhanumurthy, K.; Kale, G.; Chatterjee, S. Diffusion bonding of commercially pure titanium to 304 stainless steel using copper interlayer. *Mater. Sci. Eng. A* **2005**, *407*, 154–160. [CrossRef]
40. Zhang, Y.; Chen, Y.; Zhou, J.; Sun, D.; Li, H. Experimental and numerical study on microstructure and mechanical properties for laser welding-brazing of TC4 Titanium alloy and 304 stainless steel with Cu-base filler metal. *J. Mater. Res. Technol.* **2020**, *9*, 465–477. [CrossRef]